



Title	^{13}C -NMR studies of the paramagnetic and charge-ordered states of the organic superconductor $\beta''\text{-(BEDT-TTF)}_3\text{Cl}_2 \cdot 2\text{H}_2\text{O}$ under pressure
Author(s)	Nagata, Sanato; Ogura, Takashi; Kawamoto, Atsushi et al.
Citation	Physical Review B, 84(3), 035105 https://doi.org/10.1103/PhysRevB.84.035105
Issue Date	2011-07-15
Doc URL	https://hdl.handle.net/2115/46886
Rights	© 2011 American Physical Society
Type	journal article
File Information	PRB84-3_035105.pdf



^{13}C -NMR studies of the paramagnetic and charge-ordered states of the organic superconductor $\beta''\text{-(BEDT-TTF)}_3\text{Cl}_2\cdot 2\text{H}_2\text{O}$ under pressure

Sanato Nagata, Takashi Ogura, and Atsushi Kawamoto*

Department of Quantum and Condensed Matter Physics, Graduate School of Science, Hokkaido University, Kita-ku, Sapporo, Hokkaido 060-0810, Japan

Hiromi Taniguchi

Department of Physics, Faculty of Science, Saitama University, Shimo-Ohkubo 255 Saitama, Saitama 338-8570, Japan

(Received 15 February 2011; revised manuscript received 13 April 2011; published 18 July 2011)

$\beta''\text{-(BEDT-TTF)}_3\text{Cl}_2\cdot 2\text{H}_2\text{O}$ [BEDT-TTF: bis-(ethylenedithio)tetrathiafulvalene] is superconductive under pressures, whereas the salt exhibits metal-insulator (MI) transition under ambient pressure. The insulator phase in the salt was examined using the charge density wave (CDW) phase that was obtained from band calculation. The charge-ordered (CO) state was recently proposed as the insulator phase of the salt, and the mechanism of superconductivity intermediated by charge fluctuation was suggested. We accessed ^{13}C -NMR on $\beta''\text{-(BEDT-TTF)}_3\text{Cl}_2\cdot 2\text{H}_2\text{O}$ at ambient pressure and under pressure up to 1.6 GPa. At ambient pressure, the NMR spectrum changed at approximately 100 K. Three isolated peaks appeared at low temperatures, suggesting that the CO state exists below 100 K, and spin-gap behavior was observed. By analyzing the chemical shift, the charges on the three sites were estimated as $\sim +0.4e$, $\sim +0.6e$, and $\sim +1.0e$. The ratio of peak intensity and unsymmetrical peak position suggest the CO state with some symmetry breaking. When pressure is applied, the splitting of the NMR peaks in the CO state is reduced. The salt finally exhibits superconductivity at 1.6 GPa, spin-gap behavior observed at $(T_1 T)^{-1}$ below 1.3 GPa suddenly disappears, whereas the NMR spectrum predicts that charge disproportionation coexists with superconductivity. The suppression of the spin-singlet formation observed in $(T_1 T)^{-1}$ at 1.6 GPa suggests the metallic state with the charge disproportionation and the CO instability with some symmetry breaking.

DOI: [10.1103/PhysRevB.84.035105](https://doi.org/10.1103/PhysRevB.84.035105)

PACS number(s): 71.30.+h, 74.70.Kn, 76.60.-k

I. INTRODUCTION

The superconductivity of $\kappa\text{-(BEDT-TTF)}_2\text{X}$ (BEDT-TTF: bis-(ethylenedithio)tetrathiafulvalene) as well as of high- T_c cuprates is attractive, because of the relationship between antiferromagnetic fluctuations and superconductivity.¹⁻³ In a quarter-filled electron system with the $(\text{BEDT-TTF})_2\text{X}$ composition formula, the degree of dimerization determines the properties of the insulating phase. If the dimerization is strong, the system can be regarded as half-filled and is a dimer Mott insulator. Because κ -type salts are well known to form strong dimerization of BEDT-TTF molecules, they may be considered as a half-filled system, and therefore, as dimer Mott insulators.⁴ On the other hand, if the dimerization is weak, the system can be regarded as quarter-filled, and the effective on-site and off-site Coulomb repulsive energy (U and V , respectively) cause the system to form a charge-ordered (CO) state.⁵ Some organic conductors such as α -type, α' -type, and θ -type salts⁶ dimerize weakly and are not regarded as half-filled but as quarter-filled systems. Their insulating phase is likely to be the CO state.⁷⁻¹³ Some of these salts exhibit superconductivity under applied or ambient pressure.^{14,15} It has been suggested that the mechanism of superconductivity in these salts is intermediated not by antiferromagnetic fluctuations but by charge fluctuations.¹⁶

The crystal structure of $\beta''\text{-(BEDT-TTF)}_3\text{Cl}_2\cdot 2\text{H}_2\text{O}$ is shown in Fig. 1.¹⁷ Its space group is $P\bar{1}$, and its unit cell contains three crystallographically independent molecules (A, B, and C). Whereas α -type and θ -type salts have a two column structure tilted with respect to each other, all of the molecules in this salt are almost parallel to each other and form a

stacking structure. The dimerization in the stack is as weak as in α -type and θ -type salts. It undergoes a metal-insulator transition (MIT) at $T_{\text{MI}} \sim 130$ K under ambient pressure and becomes a superconductor at 1.6 GPa with $T_c = 1.9$ K, which was confirmed by two groups (Mori *et al.* and Lubczynski *et al.*) independently.^{17,18} Another remarkable feature of this salt is that, in contrast to $(\text{BEDT-TTF})_2\text{X}$, the formal charge is not expected to be $+1/2e$ per molecule but is expected to be $+2/3e$ per molecule.¹⁹ Because its Fermi surface is one-dimensional, the MIT has been believed to originate from a charge density wave (CDW) formation by the nesting of conducting bands.^{18,20} Because the superconducting phase is adjacent to the insulating phase, it was suggested that superconductivity is mediated by the CDW fluctuation. However, x-ray experiments showed that the MIT was not accompanied by a modification of the crystal structure.²¹ Because this salt cannot be regarded as a half-filled electron system and the dimerization is not sufficiently strong, the formation of a CO in the insulating phase is likely.

Yamamoto *et al.* recently reported comprehensive optical studies of β'' -type salts.⁸ The optical measurements are mainly sensitive to the electric charge. The linewidth of the optical spectrum was very broad at 300 K. With decreasing temperature, a broad peak split into two prominent peaks. The resistivity increases steeply below 100 K because of which the peak becomes sharper. These results suggested that the CO transition occurs at approximately 100 K. Furthermore, the pressure dependence of the Raman spectrum at 10 K showed that the splitting of the spectrum decreased with increasing pressure, and they claimed that charge inhomogeneity

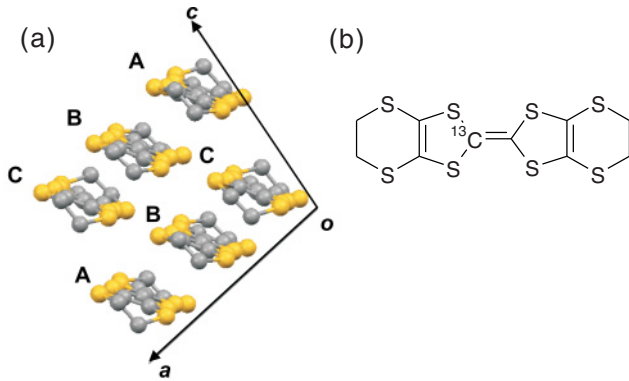


FIG. 1. (Color online) (a) Crystal structure of β'' -(BEDT-TTF)₃Cl₂·2H₂O¹⁷ (b) Molecular structure of BEDT-TTF-¹³C

remained even at the critical pressure of superconductivity. The characterization of the insulating phase is necessary for understanding the mechanism of superconductivity. For this purpose, nuclear magnetic resonance (NMR) measurement is one of the best tools. NMR on $I = 1/2$ nuclei is sensitive to the magnetism on conducting electrons. Therefore, NMR is complementary to optical observations. Moreover, NMR can directly obtain information on the charge as chemical shift data. If the CO state arises, a separation of the NMR spectrum corresponding to the charge-rich and charge-poor sites on the BEDT-TTF molecule is expected, observed in α -(BEDT-TTF)₂I₃, α' -(BEDT-TTF)₂IBr₂, and θ -(BEDT-TTF)₂RbZn(SCN)₄.^{12,13,22,23} If a CDW arises, it is very likely to be an incommensurate CDW, and the NMR spectrum will not separate but only broaden slightly.

The peak splitting observed in optical spectroscopy cannot distinguish a static charge separation from a dynamic one owing to its fast time resolution of ~ 1 THz. In contrast, NMR spectra actually detect the static properties below the NMR linewidth of ~ 1 kHz. Moreover, the ratio of peak intensity in the optical spectrum does not simply correspond to the abundance ratio of each site. The peak intensity in NMR is directly proportional to the number of corresponding sites, and the NMR spectrum provides information on the abundance of charge-rich and charge-poor sites. The magnetic gap can also be detected by the Knight shift and the spin-lattice relaxation rate T_1^{-1} . In order to elucidate the charge state in the insulating phase, we have conducted ¹³C-NMR measurements. Moreover, to investigate what type of changes occur under pressure, we also performed ¹³C-NMR measurements under pressures up to 1.6 GPa.

II. EXPERIMENTAL

To avoid the Pake doublet problem, we added ¹³C isotopes on only one side of the central carbon sites of the BEDT-TTF molecules shown in Fig. 1(b).^{24,25} This enriched molecule enables us to analyze the NMR shift and provide a quantitative interpretation of the spin-lattice relaxation rate. The salt was prepared by the electrochemical method by using [*n*-Bu₄N]CoCl₄ as the electrolyte.¹⁷ NMR measurements were performed with decreasing temperature under a field of 9.4

T and under pressures ranging from ambient to 1.6 GPa by using a clamp cell made of BeCu alloy. Daphne oil 7373 was used as the pressure medium. The pressure was calibrated using the resistance of a Manganin wire at room temperature. A magnetic field was applied perpendicular to the conducting layer (0,1,0); the corresponding resonance frequency was 100.7 MHz. The NMR spectrum was obtained by fast Fourier transformation (FFT) of the spin-echo signal following a conventional $\pi/2-\pi$ pulse sequence by using a single crystal. The spin-lattice relaxation rate was measured by the saturation recovery method on 15 pieces of crystal (~ 3.5 mg) stacked on the (0,1,0) plane. The static susceptibility was measured by a SQUID magnetometer, and the spin susceptibility χ_s was estimated after the diamagnetic correction.

III. NMR SHIFT OF ORGANIC CONDUCTORS

The NMR shift δ is generally expressed as the sum of the chemical shift σ , which is because of the coherent shielding current of the molecular orbital and the Knight shift, $K = A \chi_s$ caused by spin magnetization. Here, A is the hyperfine coupling constant and χ_s is the spin susceptibility. Because spin magnetization gives rise to the magnetic field via exchange and dipole interaction, K is sensitive not only to the magnetization on the target molecule but also to the crystallographic environment. In contrast, σ is sensitive only to the orbital terms of the target molecule. Owing to the anisotropy of the molecule and the crystal system, σ and A are expressed by the chemical shift tensor $\overleftrightarrow{\sigma}$ and the hyperfine coupling tensor \overleftrightarrow{A} as $\sigma = \vec{h} \overleftrightarrow{\sigma} \vec{h}$ and $A = \vec{h} \overleftrightarrow{A} \vec{h}$, respectively. Here, \vec{h} is the direction cosine of the external field in the molecular coordinate system. We used the enriched molecule on a single side of the central C=C carbons. When the molecule is not on an inversion center, the two central C=C carbons are inequivalent, and their Knight shift tensors differ. In contrast, their chemical shift tensors are almost the same because the chemical shift is mainly because of the charge on the molecular orbitals.

A unit cell contains one crystallographically independent molecule and both central C=C carbons are crystallographically independent in θ -(BEDT-TTF)₂RbZn(SCN)₄ at room temperature. Therefore, signals from two ¹³C nuclei on the same molecule have been observed.¹² When the CO transition occurred, two molecular sites in a unit cell, the charge-rich and charge-poor sites, became crystallographically independent. Therefore, we could observe four signals from two ¹³C nuclei in the charge-poor site and two ¹³C nuclei in the charge-rich site. At low temperature, the spin susceptibility diminished because of the spin-Peierls transition, the contribution from the Knight shift disappeared, and only the chemical shift contributed to the NMR shift, $\delta \simeq \sigma$. Because the chemical shift depends on the charge of a molecular orbital and is insensitive to the position of the central C=C carbons, only two signals from the charge-poor site and charge-rich sites are observed. Therefore, the NMR shift provides important information about the CO state, especially in nonmagnetic phases.

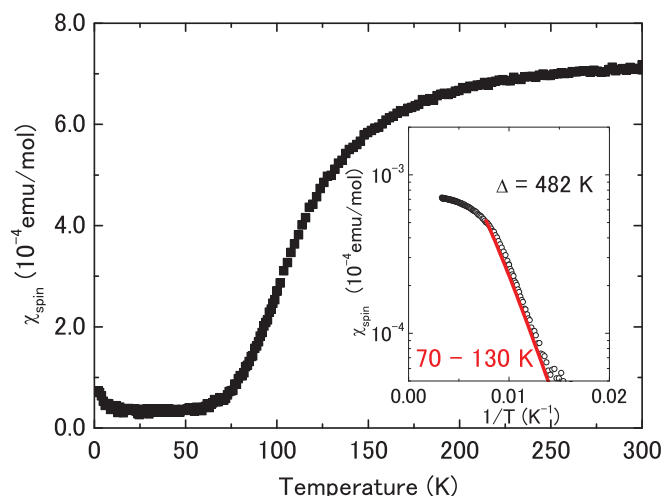


FIG. 2. (Color online) Temperature dependence of the spin susceptibility of β'' -(BEDT-TTF)₃Cl₂·2H₂O (Inset: Fitting with the dimer model.)

IV. RESULTS AND DISCUSSION

A. Static susceptibility

Figure 2 shows the temperature dependence of χ_s for the polycrystal sample. We observed a temperature-independent Pauli paramagnetic susceptibility above 150 K. This result is consistent with the metallic behavior of the electrical conductivity above 150 K. The spin susceptibility of 7.0×10^{-4} emu/mole at 300 K corresponds to the susceptibility of 2.3×10^{-4} emu/mole f.u. per one BEDT-TTF and this value is comparable to that of κ -(BEDT-TTF)₂X salt (2.5×10^{-4} emu/mole f.u.). The spin susceptibility starts to decrease sharply at approximately 150 K and becomes non-magnetic at approximately 50 K. Moreover, the preliminary measurement of the aligned crystal does not exhibit significant anisotropy. These results predict that the decrease in susceptibility is not because of the antiferromagnetic transition but because of the spin-singlet formation. The absolute value of χ_s per BEDT-TTF molecule is comparable to those for other (BEDT-TTF)₂X salts. We estimate the spin-gap energy phenomenologically by the fitting with the dimer model, $\chi = \frac{C}{k_B T} [1/(3 + e^{\Delta/k_B T})]$, as shown in the inset of Fig. 2 where k_B is the Boltzmann constant and C is a scale constant. As a result, we obtain a gap of $\Delta \sim 482$ K. On many CO salts, the spin susceptibility has been found to decrease with CO formation.^{13,23}

B. NMR shift under ambient pressure

Figure 3 shows the temperature dependence of the ¹³C-NMR spectrum from 295 K to 45 K at ambient pressure. With the exception of a signal from grease at ~ 30 ppm, a four-peak spectrum was observed at 295 K; the ratio of the peak's intensities is estimated at approximately 1:2:2:1. Because the optical spectrum suggested a homogeneous charge distribution, $\rho = 2/3$, at room temperature, the NMR spectrum is interpreted as arising from six signal of two C=C sites each in three independent molecules with different hyperfine coupling constants A_i . With decreasing temperature, the

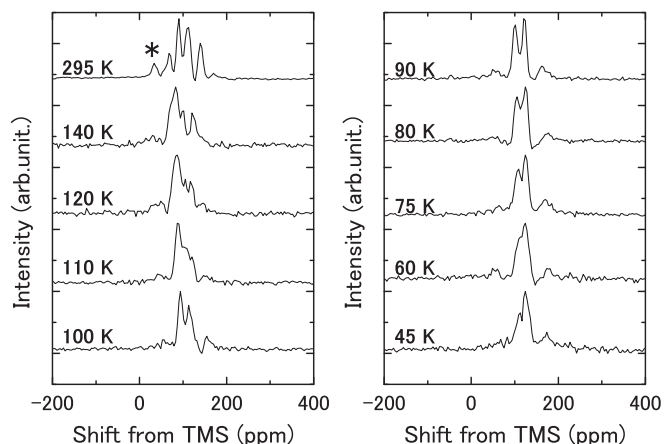


FIG. 3. NMR spectra of β'' -(BEDT-TTF)₃Cl₂·2H₂O at ambient pressure. The asterisk denotes a signal from grease.

peaks shifted gradually to ~ 100 ppm and broadened. The broadened spectrum changed abruptly at 100 K, and three distinct peaks were observed. These behaviors are characteristics of the CO transition and have been observed in θ -(BEDT-TTF)₂RbZn(SCN)₄ and α' -(BEDT-TTF)₂IBr₂.^{12,23} In optical spectroscopy, peak splitting was also clearly visible at approximately 100 K, suggesting dynamic or static charge disproportionation. Considering the sharp NMR peaks below 100 K, the splitting of the NMR peaks predicts static charge disproportionation at approximately 100 K. Figure 4 shows the temperature dependence of the NMR shift of each peak. The three peaks visible at 100 K shifted to higher values with decreasing temperature and did not show significant changes below 80 K where the spin susceptibility almost vanished and the NMR shift δ is almost determined by σ . Hence the number of peaks at low temperature corresponds to the number of molecules with different charge states.

It is important to discuss the degree of charge disproportionation and the CO pattern in order to understand the

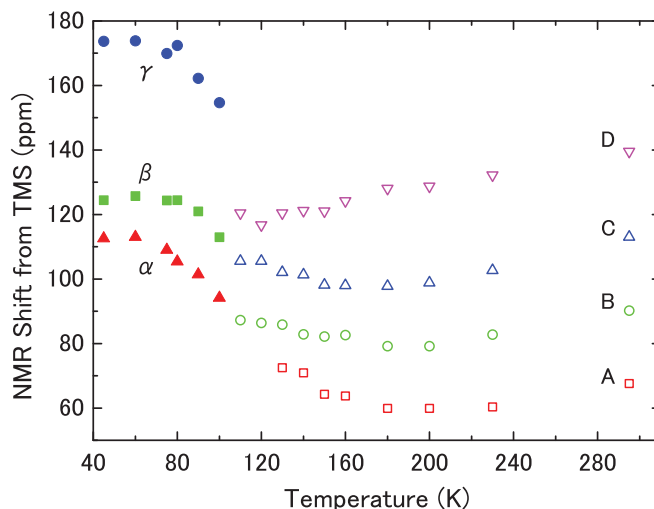


FIG. 4. (Color online) Temperature dependence of NMR shift of β'' -(BEDT-TTF)₃Cl₂·2H₂O at ambient pressure. Peak labels correspond to those in Fig. 3.

electrical properties of this salt. Considering the NMR results for θ -(BEDT-TTF)₂RbZn(SCN)₄ and α -(BEDT-TTF)₂I₃, it has been suggested that when a magnetic field was applied parallel to the long axis of the BEDT-TTF molecule, charge-rich sites were indicated by large shifts and charge-poor sites by small shifts.^{13,26} In the current configuration, the magnetic field is applied almost parallel to the long axis of the BEDT-TTF molecule. Using the chemical shift tensor in α -(BEDT-TTF)₂I₃ in the CO state¹³ and the direction cosine of the magnetic field in the current experiment, we evaluated the relation between the charge, ρ and the chemical shift as $\sigma(\rho) = 61 + 109\rho$, assuming the disproportionation of the charge in α -(BEDT-TTF)₂I₃ as 0.75:0.25²⁷. Using this relationship, the charge distribution on β'' -(BEDT-TTF)₃Cl₂·2H₂O is estimated as $\sim +0.4$ (109 ppm), $\sim +0.6e$ (126 ppm), and $\sim +1.0e$ (174 ppm).

In case of the incommensurate CDW expected from the band structure,²⁰ NMR spectrum should be a symmetrical and continuous structure around $+0.66e$. Even if a commensurate CDW occurs, the separate peaks should be observed symmetrically around $+0.66e$. The unsymmetric peak position and distribution observed at low temperature suggest not the CDW but the CO state.

Because a unit cell contains three crystallographically independent molecules, the disproportionation may not break the crystal symmetry but simply develop among the three molecular sites. The advantage of NMR is that the peak intensity is proportional to the site ratio, whereas the intensity in vibrational spectroscopy depends on the transition moment or the scattering cross section either of which are not simply proportional to the site ratio. From the fitting of the spectrum with Lorentzians at low temperature, as shown in Fig. 5, the ratio of the intensity of the peaks is estimated as 2:3:1. Therefore, there are a unit cell contains two charge-poor sites, three slightly charge-poor sites, and one very charge-rich site. $P\bar{1}$ symmetry cannot explain the ratio of peak intensities, and the inversion center or translational symmetry must be broken.

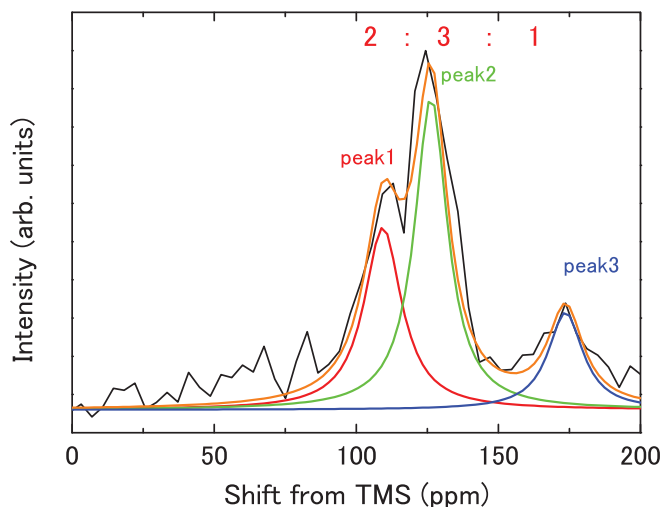


FIG. 5. (Color online) NMR spectrum of β'' -(BEDT-TTF)₃Cl₂·2H₂O at 45 K.

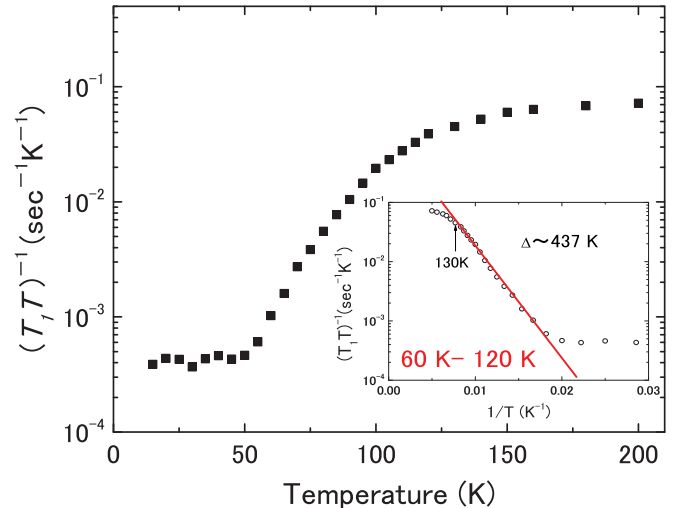


FIG. 6. (Color online) Temperature dependence of $(T_1 T)^{-1}$ of β'' -(BEDT-TTF)₃Cl₂·2H₂O at ambient pressure. (Inset: Fitting with the thermally activated model.)

C. $(T_1 T)^{-1}$ under ambient pressure

The temperature dependence of $(T_1 T)^{-1}$ for the integration of all peaks is shown in Fig. 6. Above 130 K, the spin susceptibility and $(T_1 T)^{-1}$ are almost constant, suggesting that the Korringa relationship holds. Below 130 K, $(T_1 T)^{-1}$ decreases with decreasing temperature similar to the spin susceptibility. In low temperature phase, T_1 of each peak behaves the same temperature dependence with the ratio of 1.6. To improve signal-to-ratio and compare with that under pressure, we evaluate T_1 for the integration peaks. The relaxation curve could be fitted as a single exponent function.

This spin-singlet formation should be observed in the spin-lattice relaxation rate in ¹³C-NMR. Defining the temperature T_g as that at which the gap starts to form, $T_g \sim 130$ K is almost the same as the MIT temperature T_{MI} estimated from the electrical conductivity measurement. We used thermal activation model fitting, $(T_1 T)^{-1} \propto e^{\Delta/k_B T}$, to evaluate the gap energy, $\Delta \sim 437$ K from T_1 . The value is consistent with that from the spin susceptibility.

T_g is slightly higher than the transition temperature at which the NMR and optical spectra change abruptly. The spectral broadening above 100 K in the NMR and optical spectra suggest dynamic CO fluctuation similar to that in θ -(BEDT-TTF)₂RbZn(SCN)₄ and α' -(BEDT-TTF)₂IBr₂. This fluctuation makes the magnetic gap dynamically open and scatters the conduction electrons above 100 K.

D. NMR measurement under pressure

Measurements of electrical conductivity under pressure showed that the MIT is strongly suppressed by applying pressure, and this salt exhibits superconductivity above 1.6 GPa. To inspect how the CO state changes, we conducted ¹³C-NMR measurements under pressure.

Figure 7 shows the temperature dependence of NMR spectra at 1.0 GPa. Four peaks were observed at 295 K and 1.0 GPa as well as under ambient pressure, but the splitting width of the peaks is narrower than that under ambient

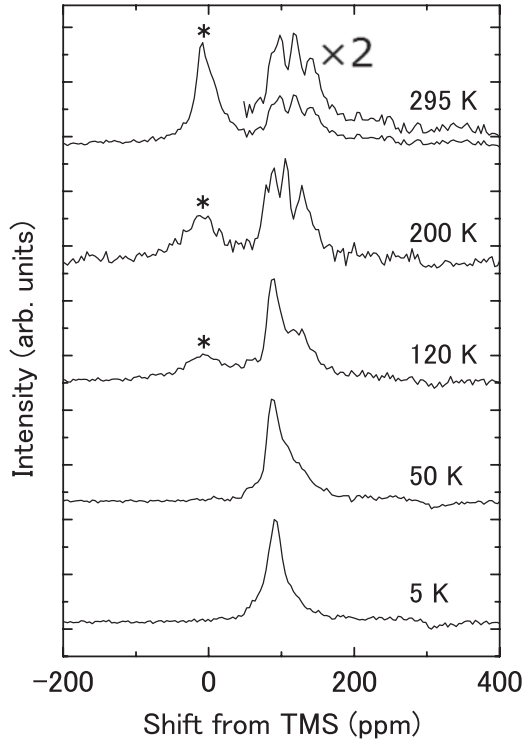


FIG. 7. NMR spectra of β'' -(BEDT-TTF)₃Cl₂·2H₂O at 1.0 GPa. The asterisk denotes the signal from Daphne 7373.

pressure. Because the splitting width $\Delta\delta \approx \Delta K$ is expressed as $\Delta K = \Delta A_i \chi_s$, this result corresponds to a reduction in the spin susceptibility with the application of pressure. Because $\Delta K_{1.0\text{GPa}}/\Delta K_{AP} = 0.75$, the spin susceptibility was reduced by 25%. The reduction can be regarded as a decrease in the density of states because of an increase in the transfer integral caused by increased pressure.

The temperature dependence of $(T_1 T)^{-1}$ is shown in Fig. 8. Below 1.3 GPa, $(T_1 T)^{-1}$ was constant at high temperature and decreased at low temperature, which is similar to its behavior as under ambient pressure, suggesting that spin-gap formation also occurs under pressure. The value of $(T_1 T)^{-1}$ at high temperature decreases with increasing pressure, like the spin susceptibility. The value of $(T_1 T)^{-1}_{1.0\text{GPa}}/(T_1 T)^{-1}_{AP} = 0.5$ is consistent with $(\Delta K_{1.0\text{GPa}}/\Delta K_{AP})^2 = 0.56$. T_g and the temperature at which $(T_1 T)^{-1}$ begins to decrease drops with increasing pressure. The recovery curve could be fitted with a single exponent function at all temperatures and pressures include 1.6 GPa. Unlike κ -(BEDT-TTF)₂X salts, the development of the antiferromagnetic fluctuation is not observed in the metal phase of this salt under all pressures, suggesting that the pairing mechanism is not the antiferromagnetic fluctuations.

Although $(T_1 T)^{-1}$ did not show significant temperature dependence above T_g , the spectral shape changed remarkably with decreasing temperature. If the spin susceptibility changes with temperature, the splitting width simply changes and the total spectral shape does not change. Considering that the spin susceptibility is not expected to show significant temperature dependence from $(T_1 T)^{-1}$ above T_g , the change of the spectral shape corresponds to the disproportionation of the local spin susceptibility. Since the charge disproportionation was

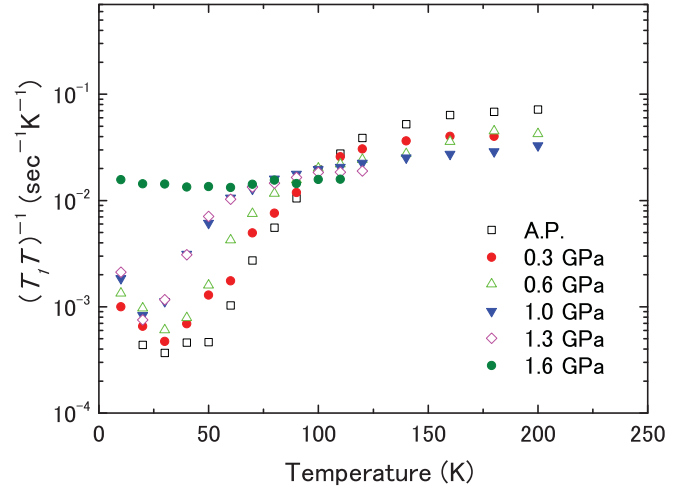


FIG. 8. (Color online) $(T_1 T)^{-1}$ of β'' -(BEDT-TTF)₃Cl₂·2H₂O under pressure.

observed above CO transition temperature in previous studies of many CO salts,^{13,28–30} the origin of the disproportionation of the local spin susceptibility is likely to the charge disproportionation.

Figure 9(a) shows the pressure dependence of T_g with T_{MI} from the electrical conductivity measurements under pressure. T_g behaves in a way similar to T_{MI} , suggesting that the CO state is also realized under pressure with spin-singlet formation. As shown in Fig. 9(b), we also estimated the gap energy at each pressure by means of thermal activation model fitting. The gap energy also decreased with increasing pressure up to 1.3 GPa. As pressure is applied, the transfer integral increases, and the itinerant-electron system is enhanced. Thus, the amplitude of the charge disproportionation is expected to become small, and the gap energy is expected to decrease. Below 20 K, at which the spin susceptibility is expected to be vanished, a broad peak was observed. This broadening is because of the disproportionation of charge. The full-width at half-maximum (FWHM) of ~ 50 ppm at 5 K is approximately half of that under ambient pressure, suggesting that the charge

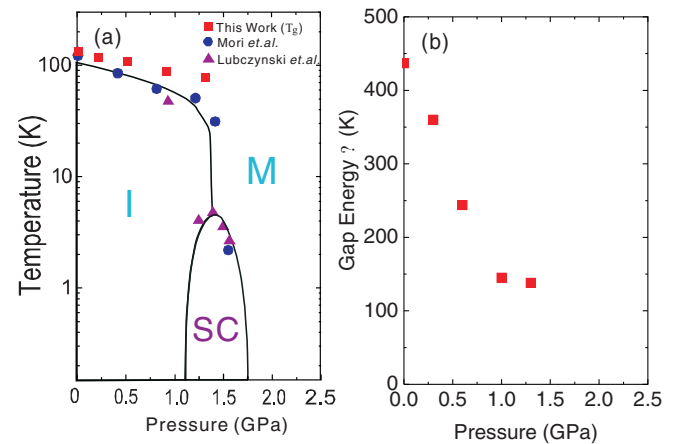


FIG. 9. (Color online) (a) Phase diagram of β'' -(BEDT-TTF)₃Cl₂·2H₂O^{18,19} and (b) pressure dependence of Δ . Horizontal axis corresponds to pressure at room temperature.

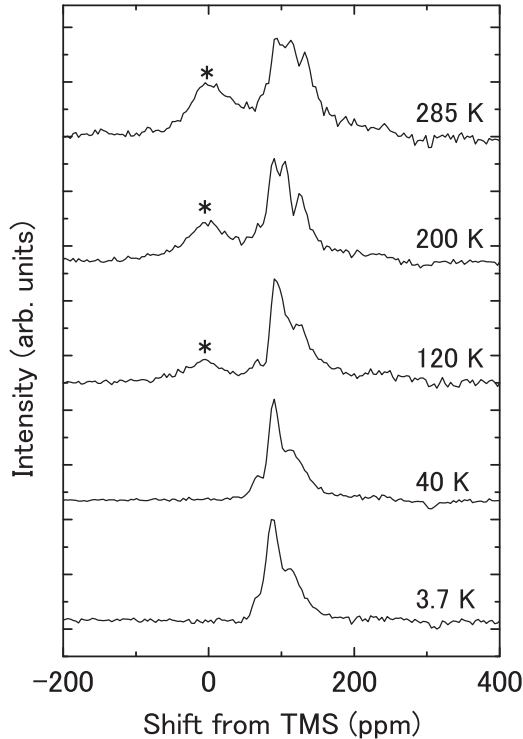


FIG. 10. NMR spectra of β'' -(BEDT-TTF) $_3$ Cl $_2$ ·2H $_2$ O at 1.6 GPa. The asterisk denotes the signal from Daphne 7373.

disproportionation is reduced by pressure; this reduction was also observed in the Raman spectra.

A most interesting problem is whether spin-gap remains or vanishes under the critical pressure. As shown in Fig. 8, $(T_1T)^{-1}$ is almost constant, as in metallic behavior, and the spin-gap vanishes at 1.6 GPa, suggesting that the CO transition with symmetry breaking was suppressed. To elucidate the mechanism of superconductivity, it is important to consider whether the system is a simple metallic state or an exotic metallic state in which an itinerant-electron system and charge disproportionation coexist. The Raman spectrum also exhibited splitting into two peaks at 1.6 GPa, but not as clearly. As shown in Fig. 10, the spectral features at 285 K are the same as those at ≤ 1.0 GPa. Because a homogeneous charge distribution is suggested, the FWHM at 285 K and 1.6 GPa does not differ greatly from that at 1.0 GPa, suggesting that the spin susceptibility is almost the same.

The temperature dependence of the spectrum shape is similar to that at 1.0 GPa above 120 K. The temperature dependence of the NMR spectra and the gapless behavior in $(T_1T)^{-1}$ predicts that charge disproportionation as observed at 1.0 GPa and just above 120 K will remain at critical pressure without spin-singlet formation. Semiconductive behavior just above T_c ¹⁹ can be examined by charge disproportionation without spin-singlet formation.

E. Charge disproportionation and magnetism in β'' -(BEDT-TTF) $_3$ Cl $_2$ ·2H $_2$ O

As previously discussed, we observed not only the charge disproportionation indicated by the Raman scattering but also the vanishment of spin-gap behavior under critical pressure

where the superconductivity occurs at low temperature. These results predict the metal phase with charge disproportionation by off-site Coulomb repulsion just above T_c . It was reported that the electrical resistivity is not simple metallic but semiconductive just above T_c .¹⁹ This behavior may connect to the metallic state with the disproportionation. Because the semiconductive behavior was also observed in β'' -(BEDT-TTF) $_4$ [(H $_3$ O)Ga(C $_2$ O $_4$) $_3$]·C $_6$ H $_5$ NO $_2$,^{31,32} it is suggested that the metal phase with charge disproportionation is the common nature of superconductive β'' -type salts.

The electron scattering mechanism with the charge disproportionation by off-site Coulomb repulsion is interesting. Considering that the mechanism of superconductivity is not antiferromagnetic fluctuations, theoretical study of the relationship between the metallic state with charge disproportionation and superconductivity is desired.

V. CONCLUDING REMARKS

We performed 13 C-NMR on β'' -(BEDT-TTF) $_3$ Cl $_2$ ·2H $_2$ O at ambient pressure and under pressure of up to 1.6 GPa. At ambient pressure, we found an abrupt change in the spectrum near 100 K. Below T_{MI} , $(T_1T)^{-1}$ shows a gap in the spin behavior of $\Delta = 437$ K, which is the same as that in the spin susceptibility. With decreasing temperature, the splitting becomes clearer, and three isolated peaks appear at low temperature. These results suggest that the CO state appears below 100 K; the charges on the three sites are estimated as $\sim +0.4e$, $\sim +0.6e$, and $\sim +1.0e$. The intensity ratio and the unsymmetrical peak position suggest not the CDW but the CO with some symmetry breaking. Above the CO transition, the spin susceptibility and $(T_1T)^{-1}$ are almost constant, suggesting Fermi-liquid behavior. By applying pressure, the splitting of NMR peaks and $(T_1T)^{-1}$ above the CO transition are reduced, corresponding to a decrease in the density of states at the Fermi energy, and the gap energy and T_g decrease. At 1.6 GPa, the salt finally exhibits superconductivity and the gap behavior suddenly disappears whereas the NMR spectrum and Raman scattering predict that the charge disproportionation and superconductivity coexist at low temperatures. The temperature independence of $(T_1T)^{-1}$ at 1.6 GPa suggests a pairing mechanism of superconductivity is not antiferromagnetic fluctuations and the metallic state with the charge disproportionation and the CO instability which requires some symmetry breaking is expected to relate to the mechanism of superconductivity.

ACKNOWLEDGMENTS

The authors wish to thank K. Kumagai, Y. Furukawa, and Y. Ihara of Hokkaido University for stimulating discussions, and T. Yamamoto of Osaka University for discussions of Raman studies. The authors also thank N. Matsunaga and K. Nomura of Hokkaido University for high-pressure measurements and T. Naito and T. Inabe of Hokkaido University for x-ray measurements. This study was supported in part by a Grant-in-Aid for Scientific Research (Grant No. 18540306) from the Ministry of Education, Culture, Sports, Science and Technology of Japan.

*atkawa@phys.sci.hokudai.ac.jp

- ¹T. Moriya and K. Ueda, *Adv. Phys.* **49**, 555 (2000).
- ²H. Fukuyama, *J. Phys. Chem. Solids* **59**, 447 (1998).
- ³M. Itaya, Y. Eto, A. Kawamoto, and H. Taniguchi, *Phys. Rev. Lett.* **102**, 227003 (2009).
- ⁴H. Urayama, H. Yamochi, G. Saito, K. Nozawa, T. Sugano, M. Kinoshita, S. Sato, K. Oshima, A. Kawamoto, J. Tanaka, T. Mori, Y. Maruyama, and H. Inokuchi, *Chem. Lett.* **1988**, 55 (1988).
- ⁵H. Seo and H. Fukuyama, *J. Phys. Soc. Jpn.* **66**, 1249 (1997).
- ⁶H. Mori, S. Tanaka, and T. Mori, *Phys. Rev. B* **57**, 12023 (1998).
- ⁷T. Kakiuchi, Y. Wakabayashi, H. Sawa, T. Takahashi, and T. Nakamura, *J. Phys. Soc. Jpn.* **76**, 113702 (2007).
- ⁸T. Yamamoto, H. M. Yamamoto, R. Kato, M. Uruichi, K. Yakushi, H. Akutsu, A. Sato-Akutsu, A. Kawamoto, S. S. Turner, and P. Day *Phys. Rev. B* **77**, 205120 (2008).
- ⁹R. Wojciechowski, K. Yamamoto, K. Yakushi, M. Inokuchi, and A. Kawamoto, *Phys. Rev. B* **67**, 224105 (2003).
- ¹⁰K. Yamamoto, K. Yakushi, K. Miyagawa, K. Kanoda, and A. Kawamoto, *Phys. Rev. B* **65**, 085110 (2002).
- ¹¹Y. Takano, K. Hiraki, H. M. Yamamoto, T. Nakamura, and T. Takahashi, *J. Phys. Chem. Solids* **62**, 393 (2001).
- ¹²K. Miyagawa, A. Kawamoto, and K. Kanoda, *Phys. Rev. B* **62**, R7679 (2000).
- ¹³T. Kawai and A. Kawamoto, *J. Phys. Soc. Jpn.* **78**, 074711 (2009).
- ¹⁴N. Tajima, A. Ebina-Tajima, M. Tamura, Y. Nishio, and K. Kajita, *J. Phys. Soc. Jpn.* **71**, 1832 (2002).
- ¹⁵A. F. Bangura, A. I. Coldea, J. Singleton, A. Ardavan, A. Akutsu-Sato, H. Akutsu, S. S. Turner, P. Day, T. Yamamoto, and K. Yakushi, *Phys. Rev. B* **72**, 014543 (2005).
- ¹⁶J. Merino and R. H. McKenzie, *Phys. Rev. Lett.* **87**, 237002 (2001).
- ¹⁷T. Mori and H. Inokuchi *Solid State Commun.* **64**, 335 (1987).
- ¹⁸W. Lubczynski, S. V. Demishev, J. Singleton, J. M. Caulfield, L. Jongh, C. J. Kepert, S. J. Blundell, W. Hayes, M. Kurmoo, and P. Day, *J. Phys. Condens. Matter* **8**, 6005 (1996).
- ¹⁹T. Mori and H. Inokuchi, *Chem. Lett.* **1987**, 1657 (1987).
- ²⁰M. H. Whangbo, J. Ren, D. B. Kang, and J. M. Williams, *Mol. Cryst. Liq. Cryst.* **181**, 17 (1990).
- ²¹J. Gaultier, S. H.-Bracchetti, P. Guionneau, C. J. Kepert, D. Chasseau, L. Ducasse, Y. Barrans, M. Kurmoo, and P. Day, *J. Solid State Chem.* **145**, 496 (1999).
- ²²Y. Takano, K. Hiraki, H. M. Yamamoto, T. Nakamura, and T. Takahashi, *J. Phys. Chem. Solids* **62**, 393 (2001).
- ²³S. Hirose and A. Kawamoto, *Phys. Rev. B* **80**, 165103 (2009).
- ²⁴M. Yamashita, A. Kawamoto, and K. Kumagai, *Synth. Met.* **133–134**, 125 (2003).
- ²⁵A. Kawamoto, M. Yamashita, and K. I. Kumagai, *Phys. Rev. B* **70**, 212506 (2004).
- ²⁶R. Chiba, thesis, Gakushuin University (2002).
- ²⁷R. Wojciechowski, K. Yamamoto, K. Yakushi, M. Inokuchi, and A. Kawamoto, *Phys. Rev. B* **67**, 224105 (2003).
- ²⁸T. Kawai and A. Kawamoto, *Phys. Rev. B* **78**, 165119 (2008).
- ²⁹Y. Yue, K. Yamamoto, M. Uruichi, C. Nakano, K. Yakushi, S. Yamada, T. Hiejima, and A. Kawamoto, *Phys. Rev. B* **82**, 075134 (2010).
- ³⁰T. Kakiuchi, Y. Wakabayashi, H. Sawa, T. Takahashi, and T. Nakamura, *J. Phys. Soc. Jpn.* **76**, 113702 (2007).
- ³¹H. Akutsu, A. Akutsu-Sato, S. S. Turner, D. Le Pevelen, P. Day, V. Laukhin, Anne-Katrin Klehe, J. Singleton, D. A. Tocher, M. R. Probert, and J. A. K. Howard, *J. Am. Chem. Soc.* **124**, 12430 (2002).
- ³²A. F. Bangura, A. I. Coldea, J. Singleton, A. Ardavan, A. Akutsu-Sato, H. Akutsu, S. S. Turner, P. Day, T. Yamamoto, and K. Yakushi, *Phys. Rev. B* **72**, 014543 (2005).